Supplemental Document

With molecular structures less vulnerable to ultraviolet radiation and suitable bandgaps for water splitting, various kinds of molybdenum disulfide (MoS_2) nanostructures have been studied as promising catalysts for photocatalytic hydrogen production. Compared with common bulk MoS_2 crystals, more accessible surface reaction sites are available on MoS_2 nanostructures for photocatalytic reactions. Nevertheless, owing to the quantum confinement of nanostructures, the capability of MoS_2 nanosheets in the absorption of visible light is intrinsically unsatisfactory. The local surface plasmonic resonance (LSPR) of AuNPs has been known able to efficiently absorb visible lights. However, whether the energy absorption by the plasmonic resonance and coupling of clustered gold nanoparticles is able to promote the capability of dispersed MoS_2 nanosheets in catalyzing hydrogen evolution reactions or not is still not clear.

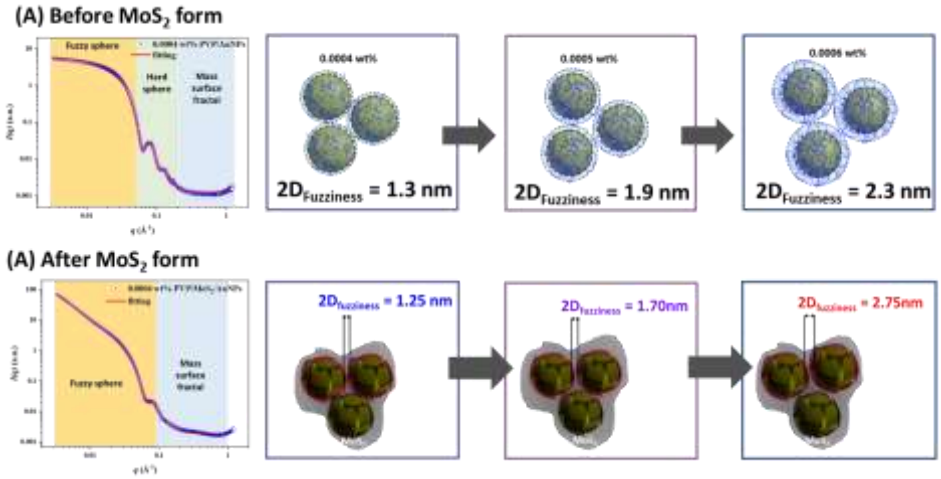

Figure. 1 (A) Small angle X-ray scattering (SAXS) data of AuNPs capping by guiding agent PVP, (B) Small angle X-ray scattering (SAXS) data of as-synthesized AuNPs/MoS_2 nanosheets hybrid nanostructure within various concentrations of PVP and corresponding fits.

The SAXS profiles have been obtained to explore the growth of MoS_2 shell on dispersed AuNPs in solutions. As shown in Figure 1, the curve fitting has been achieved also via the model of polydisperse noninteracting fuzzy spheres. The scattering intensity I(q) is strongly dominated also by the Au spheres, and the diameter of hard Au spheres is estimated around 17±3 nm accordingly. Furthermore, based on the curve fitting, the thicknesses of fuzzy MoS_2 shell around Au nanoparticles are estimated to be 0.60±0.05 nm, 0.85±0.05 nm, and 1.40±0.05 nm respectively, which is closely related to the thickness of previously existent PVP shells. As the reached thickness of MoS_2 shells is subject to the thickness of previous PVP shells, the interactions of PVP and molybdate precursors are realized to guide the growth of MoS_2 on AuNPs, rendering the PVP molecules as a kind of dispersion agent for MoS_2 nanosheets.

Following the synthesis of MoS_2 on AuNPs, the Energy dispersive X-ray (EDX) scan of prepared AuNPs/MoS_2 hybrid nanostructures has been conducted. As shown in Figure 2A, the spreading of Mo and S atoms mostly covers Au nanoparticles, and extends continuously outward beyond. Thus, the Au nanoparticles are inferred to be enclosed by synthesized MoS_2. Further illustrated by the images obtained by the high-resolution transmission electron microscope (HRTEM) (Figure 2B), crystal lattices with regular d-spacing of 0.24 nm have been observed, which reflects the presence of face-centered cubic (111) planes of gold crystals [6]. In addition, aligned (002) crystalline planes of the hexagonal 2H-MoS_2 crystals with an averaged d-spacing of about 0.65 nm have been identified. On selected-area electron diffraction (SAED) patterns obtained from individual AuNPs with MoS_2 shells (Figure 4b), bright diffraction spots selected gray circles are attributed to (111) crystallographic planes with d-spacing about 0.24 nm. Also, for the diffraction spots selected by red circles, the corresponding d-spacing is calculated to be 0.22 nm, and is explicable by the presence of (103) crystal planes of the 2H MoS_2 hexagonal

phase. In addition, the diffraction spots of (110) and (002) crystal planes of 2H hexagonal crystals have been identified. The lattice images or diffraction signals of MoS_2 crystals are only available within the area of AuNPs, and not observable in the areas between AuNPs. Hence, synthesized MoS_2 molecules in between AuNPs are inferred in amorphous status, which also emphasizes the nucleation effects of AuNPs.

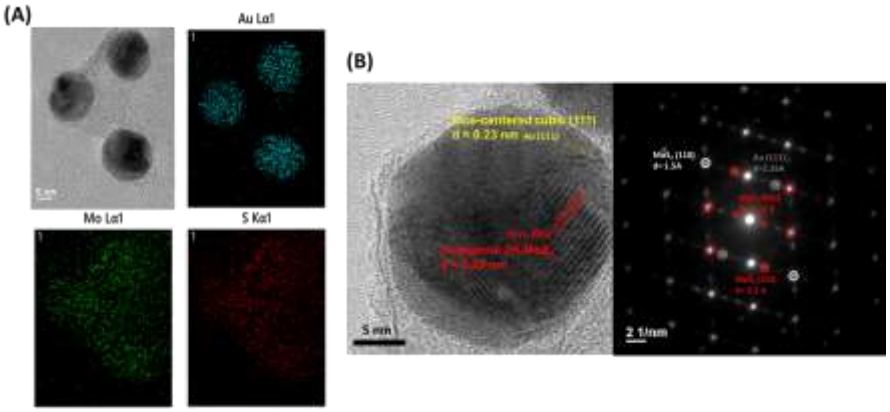

Figure 2 (A) Energy dispersive X-ray analysis (EDXA) mapping modes of the AuNPs/MoS_2 nanosheets hybrid nanostructures demonstrate that was conducted to estimate the chemical composition distribution, and (B) HRTEM images of AuNPs/MoS_2 nanosheets hybrid nanostructures showing the active sites, and interlayer (0.65 nm) of MoS_2 nanosheets, and selected-area electron diffraction (SAED) patterns obtained from the AuNPs region and MoS_2 region of AuNPs/MoS_2 nanosheets hybrid nanostructures.

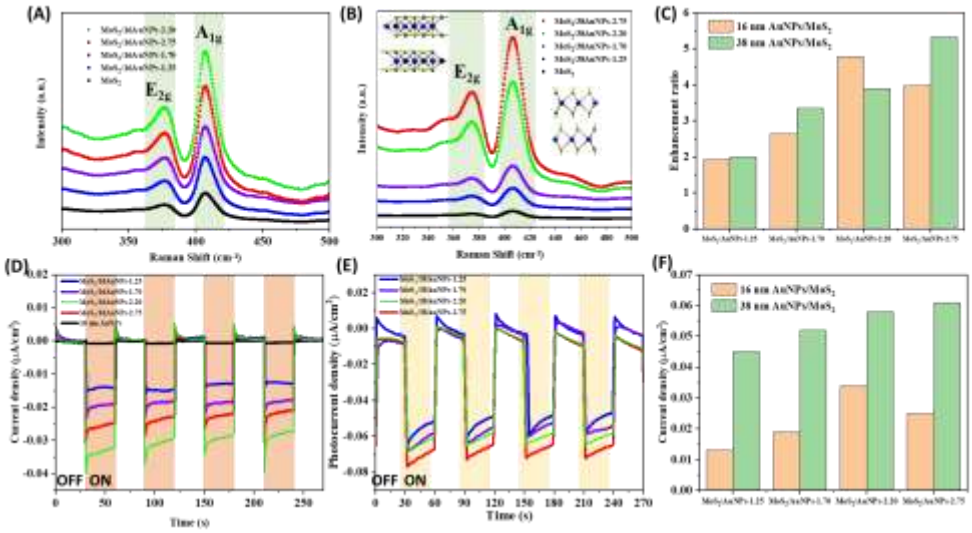

Figure 12 (A)(B)(C) Raman spectra of the pristine MoS_2, MoS_2/16AuNPs, and MoS_2/38AuNPs under 532 nm laser line. (D)(E)(F) Photocurrent density-time curves of the pristine AuNPs, MoS_2/16AuNP, and MoS_2/38AuNP under the white light illumination (bias: 0 V vs Ag/AgCl, 0.5 M Na_2SO_4, light irradiation: 400-800 nm).

Various sizes of AuNPs exhibit distinct critical edge-to-edge distances, each contributing to the optimal near-field enhancement in Figure 3. AuNPs with a diameter of 16 nm exhibit the strongest Raman enhancement at an edge-to-edge distance of 2.20 nm. In contrast, AuNPs with a diameter of 38 nm show the strongest Raman enhancement at an edge-to-edge distance of 2.75 nm. Based on the plot of photocurrent density, larger-sized AuNPs own a larger range of coupling distances and electric field strength compared to smaller-sized AuNPs. AuNPs with a size of 16 nm exhibit the strongest photocurrent at a distance of 2.20 nm. In contrast, AuNPs with a size of 38 nm show the strongest photocurrent at a distance of 2.75 nm. Therefore, it can be inferred that the optimal coupling distance for AuNPs varies with different sizes. Larger-sized particles have a larger range of coupling distances to enhance the electric field.